Preprint of M.J. Kaneshige and J.E. Shepherd.
Oblique detonation stabilized on a hypervelocity projectile.
In 26th Symposium (International) on Combustion, pages 3015–3022, Naples, 1996.

Paper Title: Oblique Detonation Stabilized on a Hypervelocity Projectile

Authors Michael J. Kaneshige
Dept. Mechanical Engineering
California Institute of Technology
Pasadena, CA 91125
phone: 626 395 4457
fax: 626 449 2677
e-mail: mikek@galcit.caltech.edu

and

J. E. Shepherd
Graduate Aeronautical Laboratory
California Institute of Technology
Pasadena, CA 91125
phone: 626 395 3283
fax: 626 449 2677
e-mail: jeshep@galcit.caltech.edu

Preference Oral presentation in **Detonations and Supersonic Flow** Colloquium

Word Count (by computer with correction for LaTeX commands)

Abstract	240
Text	3306
Figures	8 * 200 = 1600
Tables	3 * 200 = 600
Total	5506
Maximum	5500

Abstract

We present new experimental results demonstrating the initiation and stabilization of an oblique detonation by a hypervelocity projectile. Projectiles 25 mm in diameter were launched at nominal velocities of 2700 m/s into stoichiometric H_2-O_2-N_2 mixtures at pressures between 0.1 and 2.5 bar. A critical threshold in initial pressure was found to be required for the establishment of detonations. Initiation events similar to DDT in propagating waves were observed after 300 mm of travel in H_2-O_2 mixtures diluted with 25% N_2. A more direct initiation process was observed in H_2-air mixtures. A stabilized, but overdriven oblique detonation was observed in a stoichiometric H_2-air mixture at an initial pressure of 2.5 bar.

The pressure threshold can be explained in terms of competing reaction and flow quenching effects along a curving streamline in supersonic flow behind a curved shock wave. This competition can be characterized by a critical Damkohler number Da^*, which is inversely proportional to the product of wave curvature κ and reaction zone thickness Δ. Only if the reaction zone is sufficiently thin in comparison with the projectile, $Da > Da^*$, is it possible to obtain stabilized detonations. Otherwise, the reactions quench and the wave splits into a nonreactive shock wave followed by flame-like contact surface. The inverse pressure dependence $\Delta \sim P_o^{-1}$ of the reaction zone length and the scaling of the wave curvature $\kappa \sim 1/a$ with the body radius a implies the standard binary scaling relationship $P_o a =$ constant for the critical conditions of stabilization, for a given mixture composition characterized by a bimolecular rate-limiting step.

Introduction

The present experiments address the issue of the critical conditions required to stabilize an oblique detonation wave on a hypervelocity projectile fired into a premixed combustible mixture. The issue of detonation initiation and *stabilization* by hypervelocity projectiles is often confused with the numerous results on shock-initiated combustion and unsteady detonation.

Most previous experiments with projectiles, notably the often cited ones of Ruegg and Dorsey [1], Lehr [2], or Alpert and Toong [3] have been carried out under subcritical conditions and/or with projectiles traveling at less than the Chapman-Jouguet (CJ) detonation velocity. For subcritical conditions, only a limited region of shock-initiated combustion is observed behind the bow shock in the vicinity of the projectile. As the wavefront recedes from the projectile, there is a distinct point at which the chemical reactions quench and the wave appears to split into a nonreactive shock and a flame-like contact surface. Much of the analysis on these flows has been directed at understanding the striking pattern of instability waves that appears on this contact surface when the projectile velocity is near the CJ value.

Unsteady detonations have been initiated [2, 4, 5, 6] with a sufficiently large projectile traveling at sub-CJ velocities. In these cases, the projectile only plays a role in initiating the wave and ultimately is left far behind. The initiation threshold can be correlated by the empirical models of Lee [7] and Vasiljev [4], but no inferences about stabilization can be made since the detonations travel faster than the projectiles. Stabilized, planar,

oblique detonations have been created by the diffraction of planar waves in two-layer experiments [8, 9], however the problem of stability in those situations appears to be essentially different than in the case of projectiles due to the "aerodynamic" wedge created by the driving layer.

We conclude that despite three decades of research on this topic, there is scant experimental evidence for the existence of detonation waves stabilized on hypervelocity (greater than CJ) projectiles. On the other hand, there has been much theoretical analysis [10, 11] and speculation about this possibility. This situation has motivated us to reconsider this problem and carry out new experiments resulting in the successful demonstration of this phenomenon. The key to these new results is the careful choice of the mixture composition and projectile parameters, discussed in the subsequent section.

Dimensional Considerations

Consider a body with characteristic dimension a entering with velocity U into a combustible mixture. The combustible mixture is characterized by a Chapman-Jouguet detonation velocity U_{CJ} and a reference reaction zone length Δ_{CJ}. In addition, the gaseous mixture will have certain reference values of the thermodynamic and kinetic parameters such as the ratio of specific heats γ, the effective activation energy E_a, the specific energy release q, and the initial sound speed $c_\circ$. Further, it is useful to consider as parameters the characteristic time scale $t_{flow} = a/w$, where w is the (normal) postshock velocity in the projectile frame and the time scale $t_{chem} = \Delta_{\mathrm{CJ}}/w$, the time required for chemical reaction behind the bow shock (if the conditions were uniform). Finally, the

lateral (transverse) extent H (actually taken to be the effective half-width here) of the test section or guide tube is significant to understanding the results.

Based on these considerations, the significant nondimensional parameters are speed ratio, $\mathcal{U} = U/U_{\rm CJ}$; Damkohler number, $Da = t_{flow}/t_{chem}$; and facility aspect ratio, $\chi = a/H$. Critical values of these parameters will be functions of the parameters characterizing the chemical reaction and gasdynamics. The significant nondimensional state parameters are Chapman-Jouguet Mach number, $M_{\rm CJ} = U_{\rm CJ}/c_\circ$; ratio of specific heats, $\gamma = C_p/C_v$, and effective activation energy, $\theta = E_a/RT_s$.

To obtain a stabilized detonation, the projectile must be fast enough and the reaction must occur quickly compared to the flow expansion time. In addition, for the detonation wave to be initiated and sustained by the projectile, the facility aspect ratio must be sufficiently small such that wave reflections from the facility boundary are not significant. The criteria for stabilizing detonation waves on projectiles apparently are that $Da > Da^*(\mathcal{U}; M_{\rm CJ}, \theta, \gamma)$, $\mathcal{U} > 1$, and $\chi \ll 1$.

Some of these parameters are unambiguous but others require more careful consideration before they can be assigned a unique meaning. The Damkohler number in particular requires choosing a point in the flow, that is, a location on the bow shock, to evaluate the time scales. For a blunt body, a unique choice is the point directly behind the normal portion of the bow shock, leading to $Da = a/\Delta_\circ$ [12, 13, 14]. For a given composition characterized by a bimolecular rate-limiting step, this can be simplified [15, 16] to the binary scaling relationship $Da \propto Pa$, since near the nose of the projectile, $\kappa \propto 1/a$. A more detailed analysis of the reaction zone [15, 16] reveals that the local Damkohler

parameter $Da = 1/\kappa\Delta$ plays the crucial role in the quenching effect, where κ is the curvature of the wave.

An alternate manner of expressing the Damkohler number would be to use a chemical length scale based on observations of detonation instability. This is the so called cell width λ that has been used extensively in propagating detonation studies. This leads to a Damkohler-like ratio a/λ, a parameter often [17] introduced in discussing and correlating propagation detonation phenomenology such as critical diameter, initiation energy, and so forth. Detailed considerations [18] of the previous experiments reveal that the ratio a/λ must be greater than 2 to 3 for detonations to be stabilized. The present results are consistent with these considerations (see Tables 1 and 2).

These scaling ideas indicated the need for a trade-off between projectile speed and mixture sensitivity when designing the experiment. Sensitive mixtures such as stoichiometric H_2-O_2 have small cell sizes (<1 mm at 1 bar) but require very high velocity projectiles since $U_{CJ} = 2850$ m/s. Insensitive mixtures such as typical hydrocarbon fuels in air have lower CJ velocities ∼1800 m/s but much larger cell sizes, 50 to 70 mm at 1 bar. Our final design was a compromise, with a 25 mm diameter projectile that could be accelerated up to 3000 m/s so that a range of H_2-N_2-O_2 mixtures could be studied with initial pressures up to 3 bar.

See Tables 1 and 2 for values of the nondimensional detonation parameters characterizing the present experiments. The reaction zone lengths given in these tables were computed using a detailed kinetic model of the chemical reaction process, realistic thermochemistry and numerical solutions of the oblique detonation structure equations as

described in Shepherd [18]. The cell widths were taken from the literature[17].

Facility and Procedures

The experiments reported here were conducted in the T5 shock tunnel laboratory of the Graduate Aeronautical Laboratories at Caltech. T5 was converted to a gas gun (see Fig. 1) by which 10 g projectiles may be launched at velocities greater than 3000 m/s.

The inside cross-section of the test section was 152 mm square. The reactants in the test section were isolated from the dump tank and target assembly vacuums before each experiment by mylar diaphragms that sealed the 76 mm diameter openings. Three PCB dynamic pressure transducers were mounted in ports along one wall. Two pairs of small optical ports along the sides were equipped with diode lasers and photodiodes for measurement of projectile velocity. A pair of larger optical windows was used for photography. A third laser beam for projectile velocimetry was transmitted diagonally through the optical windows. The windows had a 165 mm diameter clear aperture, allowing visualization of part of the top and bottom of the test section. The inside of the test section was 762 mm long. It was capable of containing detonation pressures above 100 atm.

The photographic system was adapted from the standard T5 setup. A Q-switched Nd:YAG laser pulse was expanded and sent as a collimated beam through the test section, condensed, and imaged on a film sheet. The condensed beam was filtered to reduce the effect of thermal emission. With this setup, we created shadowgraphs and differential interferograms.

Each experiment began with the firing of T5. The high enthalpy gas created at the end of the shock tube accelerated the 25 mm diameter nylon sphere to about 2700 m/s. The projectile broke an electrical wire in the dump tank, triggering the data acquisition electronics. As the projectile passed through the test section, arrival times at the photodiode stations and the transient pressure at the transducer stations were recorded. After a delay from the break wire signal, estimated to place the projectile in the center of the window, the photograph was taken by Q-switching the Nd:YAG laser. The kinetic energy and momentum of the projectile were dissipated in a stack of aluminum plates and honeycomb in the target section. This event generated a blast wave in the test section stronger than the detonation unless the target was evacuated before the experiment.

Results

Two sets of experiments (a total of 37 tests) were performed with different reactant mixtures and with a single nominal projectile velocity. The Damkohler number was controlled by varying the initial pressure ($t_{chem} \sim P_{\circ}^{-1}$ for the present mixtures). In this fashion, the Damkohler number was varied over an order of magnitude for both reactant mixtures. This resulted in a range of phenomena that, in order of increasing initial pressure were:

1. No apparent reaction, bow shock resembled inert case.

2. Partial reaction near the front of the wave, with quenching of the reaction that created a zone of shocked but unreacted gas.

3. A nonsteady initiation event caused by interaction of the shock wave with the confinement.

4. Prompt initiation of detonation with an oblique wave extending outward to the boundaries of the confinement.

Although the amount of data is sparse and the variety of phenomena observed is rich, the results are reproducible. Duplicate experiments yield nearly identical results in almost all cases. In particular, the distinction between detonation (event 3 or 4) and quenching (1 or 2) is quite crisp and consistent. A summary of selected experiments and the resulting combustion events is given in Table 1.

Differential interferometry was used for visualization in the first set of experiments, using $2H_2+O_2+N_2$ mixtures. Shadowgraphy was employed during the second set of experiments, involving a stoichiometric mixture of H_2 and air. Uncertainty in the projectile velocity (photographic timing was accomplished with a programmable delay after the break wire signal) resulted in variation of the position of the projectile in the photographs.

In all experiments, the wall pressure was measured at three points along the test section. The arrival of the projectile was also recorded at three locations (by interruption of diode laser beams). Differences observed between the apparent wave speeds (U_{wave1} and U_{wave2}, see Table 1) and wave shapes recorded at different locations (Fig. 2) indicated unsteady behavior in the flow.

A pressure range from 0.100 to 1.000 bar was investigated in the first set of experiments (with a mixture $2H_2+O_2+N_2$). Details can be found in Bélanger et al. [19]. At

the lowest pressure (0.1 bar), a small amount of reaction was observed near the nose of the projectile. At a higher pressure of 0.250 bar, an extraordinary transient event was observed (Fig. 3). Near the projectile, the appearance of the bow wave indicated shock-induced combustion, with the reaction zone decoupling from a non-reactive shock about two diameters from the projectile. A less curved secondary wave was observed behind the projectile. This seems to indicate an explosion in the partially reacted gases behind the projectile and therefore a deflagration to detonation transition (DDT) in progress. At even higher pressure (0.50 and 1.0 bar), an overdriven detonation preceded the projectile (Fig.4). This wave was clearly a detonation, as indicated by the pressure traces and the cellular structure plainly visible behind the wave. However, the wave speed, geometry and pressure were inconsistent with a steady process.

A larger range (0.100 to 2.560 bar) of pressure was examined in the second set of experiments carried out with a less sensitive mixture $2H_2+O_2+3.76N_2$. At 0.100 bar, the bow wave did not show any sign of combustion (see Fig. 5). At 0.421 bar, a clear example of shock-induced combustion with reaction failure and reaction zone detachment was observed (Fig. 6). Evidence of the lack of reaction in this region was provided by a debris particle visible in the lower half of the image. Turbulent flow and strong refraction characteristic of combustion were observed in the portion of the particle wake behind the bow shock in the region of shocked but non-combusted reactants.

An asymmetric wave shape occurred at 1.710 bar, suggesting proximity to a transition between two types of phenomena (Fig. 7). In the lower half of the picture, the bow wave was curved and the reaction zone detached, apparently at a kink in the wave. The wave

was straight in the upper half of the picture, suggesting that the wave was self-supporting. The scale of the cellular structure in the wave shows the cell size to be comparable to the projectile radius. The bow wave at 2.560 bar initial pressure was straight over a segment between the projectile nose and a Mach reflection at the wall (Fig. 8). This wave was clearly a stabilized oblique detonation. Relatively fine cellular structure was visible behind the wave, and the wave angle indicated that the wave was slightly overdriven but much closer to a steady configuration than in the first set of experiments.

Discussion

Notable features of the experimental results are the existence of a critical pressure threshold for initiating a detonation in both cases, the nearly planar detonation wave shape for mixture 1 and the definitive oblique detonation wave observed in mixture 2.

The two sets of experiments resulted in dramatically different detonation wave shapes. A distinct oblique wave was observed in mixture 2, whereas the detonations observed for mixture 1 were nearly normal. Both wave angles are inconsistent with steady CJ waves, (see the wave angles $\beta_{\mathrm{CJ}} = \sin^{-1}(U_{\mathrm{CJ}}/U)$ in Table 2). However, while the straight portions of the detonations in mixture 2 were only slightly overdriven, the entire wave in mixture 1 was overdriven.

Major differences that could account for this variation are the speed ratio U/U_{CJ} and the reactivity of the mixtures. In set 1, the projectile velocity was only 12.5% higher than the detonation velocity, whereas in set 2, the projectile velocity was 40% higher than the CJ velocity (see Table 2).

Apparently, when the CJ speed is closer to the projectile speed, it takes longer for the initiation transient to die down and for the wave shape to relax to a steady state configuration. This is related to the observations of DDT-like processes occuring in the quenched gas region. After the unsteady explosion wave observed in Fig. 3 diffracts over the projectile, an overdriven detonation will be produced. We speculate that the nearly-planar wave observed in Fig. 4 is photographed immediately after such an event. We expect that this wave will decay and eventually reach a configuration similar to Fig. 8, since overdriven waves are susceptible to overtaking disturbances [20]. The effect of overdrive in Fig. 8 is much less pronounced since the CJ-wave angle is 16° lower and the initiation processes apparently occur more promptly. The full explanation requires further experimentation to resolve the initiation transient.

Quenching

One of most striking features of the current results is the dramatic change in the wave shape and pressure histories when a critical pressure threshold is exceeded, (see Fig. 2 and compare Figs. 6 and 8). We interpret this transition as the stabilization of the detonation wave on the projectile. The critical conditions for stabilization are those for which the "splitting" of the shock-reaction zone structure, observed in Fig. 6 and the lower half of Fig. 7, just occurs. Gilinskii and Chernyi [15] were the first to consider this process in detail and identified the Damkohler parameter Pa as the controlling factor for a given composition.

Gilinskii and Chernyi determined the critical conditions by numerically solving for the

flow in the vicinity of the body. An alternative procedure is to consider the local influence of the wave curvature on the processes in the reaction zone. From this perspective, the quenching process is a result of the competition of the flow expansion and chemical energy release in the region immediately behind the curved shock wave. The flow is undergoing adiabatic expansion because of the streamline curvature in a supersonic region behind a curved shock front.

This is exactly the same physical effect that causes freezing of dissociation behind curved bow shocks in hypervelocity flow over blunt bodies [16]. The structure of the reaction zone behind a straight oblique detonation [18] can be extended to the case of a weakly-curved ($\kappa\Delta << 1$) wave using the analysis of Hornung [16], which is based on the thin-layer equations for two-dimensional (planar) hypersonic flow. A quenching criterion can be obtained by carrying out an asymptotic analysis of the temperature variation along a streamline.

The results of this analysis show that the reaction is just quenched when the wave curvature κ exceeds the critical value κ_c. This critical value is given by $\kappa_c = 1/\theta\Delta B$, where B is a function of wave angle, freestream velocity and the thermodynamic properties of the gas. This critical curvature is a strong function of shock strength and scales directly with the initial pressure $P_\circ$ for second-order reactions since $\Delta \sim P_\circ^{-1}$. The critical curvature increases with increasing shock strength, reaching infinity at the point on the oblique shock where the downstream flow is sonic. The minimum value of κ_c occurs near the point on the wave for which the normal velocity is close to the CJ condition.

The behavior observed in our experiments can be classified as follows: 1) subcritical,

$\kappa_c < \kappa_{wave}$ for sufficiently small normal velocities, quenching occurs; 2) critical, $\kappa_c = \kappa_{wave}$ at the CJ point, this is the critical condition for oblique detonation stabilization; and 3) supercritical, $\kappa_c > \kappa_{wave}$ for all values of $U_n > U_{\mathrm{CJ}}$, quenching never occurs, the oblique detonation is always stabilized.

Conclusions and Summary

We have presented our experimental evidence for oblique detonations stabilized on projectiles. We observe transition from quenched reaction to oblique detonation with increasing initial pressure in the reactants. We present experimental evidence of this transition and argue that the parameter $\kappa\Delta$ controls the transition.

Nonsteady processes were prominent in the present experiments. Not only does a transient take place when the projectile enters the combustible test gas, but apparently a long time must elapse to get the flow to settle into a configuration that could be described as steady state. No truly steady-state like configurations were observed in the current experiments. We conclude that interpreting snapshots of potentially nonsteady events may be quite misleading and further experimentation is needed to clarify the initiation process.

Acknowledgments

We thank Hans Hornung for his encouragement and the use of T5, Jacques Bélanger for building the gun, and Bahram Valiferdowsi for running T5. This material is based upon work supported under a National Science Foundation Graduate Research Fellowship and the Powell Fund of the California Institute of Technology.

References

1. Ruegg, F. W., *Journal of Research of the National Bureau of Standards - C. Engineering and Instrumentation* **66C**, 51-58 (1962).

2. Lehr, H. F., *Astronautica Acta* **17**, 589-597 (1972).

3. Alpert, R. L. and Toong, T. Y., *Astronautica Acta* **17**, 539-560 (1972).

4. Vasiljev, A. A., *Shock Waves* **3**, 321-326 (1994).

5. Bendick, W. B., in **Fuel-Air Explosions** (J.H.S. Lee and C.M. Guirao, Eds.), Waterloo Press, 1982, p. 507.

6. Higgins, A. J. and Bruckner, A. P., *Fifteenth International Colloquium on the Dynamics of Explosions and Reactive Systems*, Boulder, CO, 1995. See also Higgins, A. J. and Bruckner, A. P., AIAA-96-0342, 1996.

7. Lee, J. H. S. *Zeldovich Memorial Conference on Combustion*, Voronovo, Russia, 1994.

8. Dabora, E. K., Desbordes, D., Guerraud, C., Wagner, H. Gg. *Prog. Aero. Astro.* **133**, 187-204 (1991).

9. Liu, J.C., Liou, J.J., Sichel, M., Kaufmann, C. W., and Nicholls, J. A. *21rst Symposium (International) on Combustion*, The Combustion Institute, 1987, pp. 1639-1647.

10. Chernyi, G. G., in **Problems of Hydrodynamics and Continuum Mechanics**, SIAM, Philadelphia, PA, 1969, 145-169.

11. Pratt, D. T., Humphrey, J. W., and Glenn, D. E., *Journal of Propulsion* **7**, 837-845 (1991).

12. Sichel, M. and Galloway, A. J., *Astronautica Acta* **13**, 137-145 (1967).

13. Hornung, H. G., *Journal of Fluid Mechanics* **53**, 149 (1972).

14. Wen, C. Y. and Hornung, H. G. *Journal of Fluid Mechanics* **299**, 389-405 (1995).

15. Gilinskii, S.M. and Chernyi, G.G. *Fluid Dynamics* **3**(1), 12-19 (1968).

16. Hornung, H. G., *Journal of Fluid Mechanics* **74**, 143-159 (1976).

17. Lee, J.H.S., *Ann. Rev. Fluid Mech.* **17**, 311-336 (1984).

18. Shepherd, J.E., in **Combustion in High-Speed Flows** (J. Buckmaster, et al., Eds.), Kluwer Academic Publishers, 1994, pp. 373-420.

19. Bélanger, J., Kaneshige, M. J., and Shepherd, J.E. in **Proceedings of the 20th ISSW**, to be published 1996.

20. Gilinskii, S.M. and Zapryanov, Z. D. *Fluid Dynamics* **2**(3), 90-97 (1967).

Table 1. Summary of T5 detonation experiments. Mixture 1: $2H_2$+O_2+N_2 and mixture 2: $2H_2$+O_2+$3.76N_2$. U_{wave1} and U_{wave2} are the apparent wave speeds computed from the detonation or shock arrival times at each pair of pressure transducers.

Mix	P_i (Bar)	U (m/s)	U_{wave1} (m/s)	U_{wave2} (m/s)	T5 Shot	Fig.	Δ_{CJ} μm	Δ_0 μm	Result
1	0.100	2690	2380	3200	865		667	233	shock-ind. comb.
1	0.250	2830	2580	3200	1012	3	253	70	DDT
1	0.500	2560	3460	2860	1010		120	60	detonation
1	1.000	2820	3060	3020	862		66.7	14	detonation
1	1.000	2930	3060	3110	863	4	66.7	14	detonation
2	0.100	2593	1670	2580	1021	5	1667	180	nonreactive
2	0.421	2683	2520	2710	1015	6	367	30	rn. zone decoup.
2	0.853	2880	2860	2780	1016		199	45	rn. zone decoup.
2	1.710	2720	3460	2980	1018	7	140	8.3	transition
2	2.560	2653	3510	4120	1020	8	160	7.0	detonation

Table 2. Nominal detonation parameters. Based on a projectile speed $U = 2700$ m/s and radius $a = 12.7$ mm. Mixture 1: $2H_2$+O_2+N_2 and mixture 2: $2H_2$+O_2+$3.76N_2$. Facility aspect ratio, χ, was fixed at 0.17

Mix	P_0 (bar)	U_{CJ} (m/s)	$\mathcal{U}$	β_{CJ} (deg)	a/Δ_{CJ}	a/Δ_0	λ_{CJ} (mm)	a/λ_{CJ}
1	0.100	2300	1.17	58.4	18.7	53.6	13	0.98
1	1.000	2400	1.13	62.7	187	893	3.2	4.0
2	0.100	1920	1.41	45.2	7.5	69.4	35	0.36
2	2.560	1990	1.34	47.4	78.1	1785	5.7	2.2

Figure Captions

Figure 1 Illustration of the experimental apparatus. The 3 meter long launch tube is mounted to T5 at the nozzle throat, at the upstream end of the dump tank, and extends into the dump tank.

Figure 2 Pressure plots from the H_2+O_2+3.76N_2 experiments, with projectile trajectories computed from diode laser - photodiode data overlayed. Projectile velocity remained constant within the test section, within measurement error.

Figure 3 T5 Shot 1012. Differential interferogram of projectile moving at 2800 m/s in 2H_2+O_2+N_2 at 0.250 bar initial pressure. Bow wave shows shock-induced combustion followed by a quenching event. An explosion in the partially reacted gases appears as a second wave behind the projectile. The dark feature in the upper center is a "clamshell" fracture in one of the windows.

Figure 4 T5 Shot 863. Differential interferogram of projectile moving at 2900 m/s in 2H_2+O_2+N_2 at 1.000 bar. Cellular structure is promeniently visible behind the leading, nearly-normal detonation front. Other features are shock waves produced by boundary separation on sphere and wake recompression shocks.

Figure 5 T5 Shot 1021. Shadowgraph of projectile moving at 2600 m/s in 2H_2+O_2+3.76N_2 at 0.100 bar. No combustion is apparent.

Figure 6 T5 Shot 1015. Shadowgraph of projectile moving at 2700 m/s in 2H_2+O_2+3.76N_2 at 0.421 bar, showing shock-induced combustion that terminates in wave-splitting (quenching) event with a flame-like contact surface separating from a

non-reactive shock.

Figure 7 T5 Shot 1018. Shadowgraph of projectile moving at 2700 m/s in $2H_2+O_2+3.76N_2$ at 1.710 bar. Asymmetry of the bow wave indicates that the event is transitional. The upper half is approximately stabilized and overdriven, while quenching occurs in the lower half.

Figure 8 T5 Shot 1020. Shadowgraph of projectile moving at 2700 m/s in $2H_2+O_2+3.76N_2$ at 2.56 bar with a stabilized overdriven detonation wave and Mach reflections at the walls. The curved feature just behind the projectile is associated with the interaction of the conical wave with the square walls of the test section. Reflected waves (at 45°) can be observed emerging from the triple points

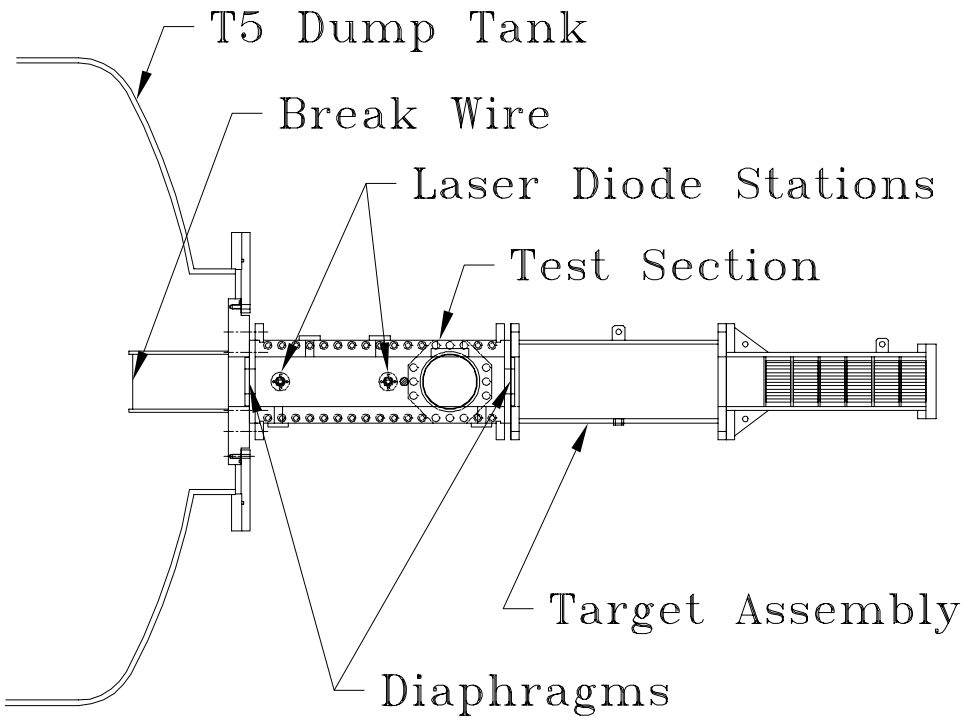

Figure 1.

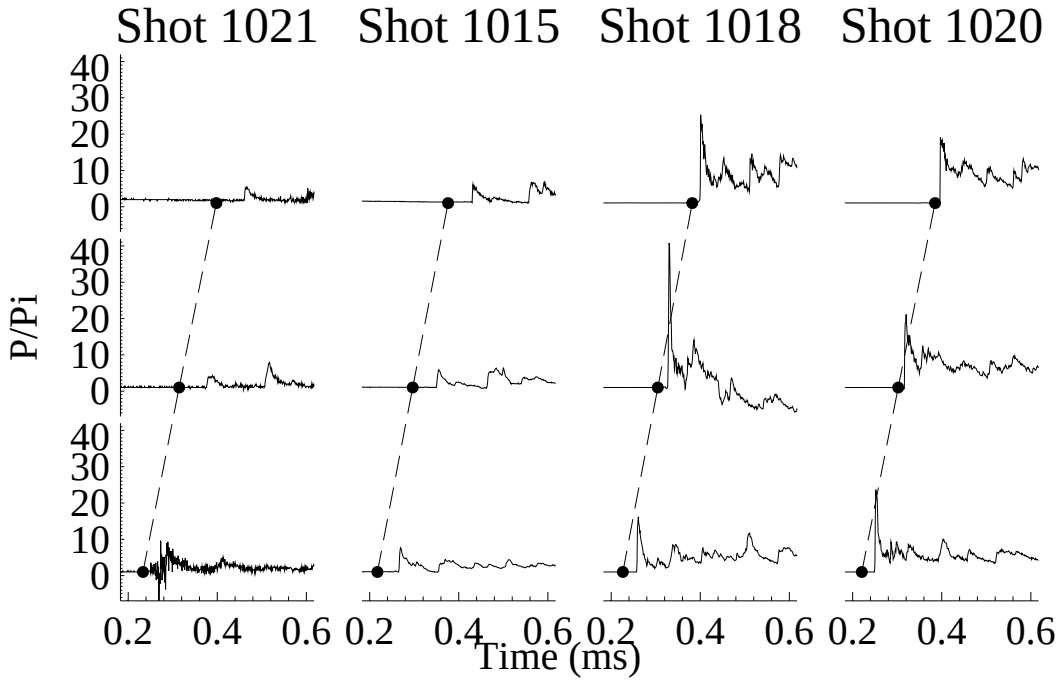

Figure 2.

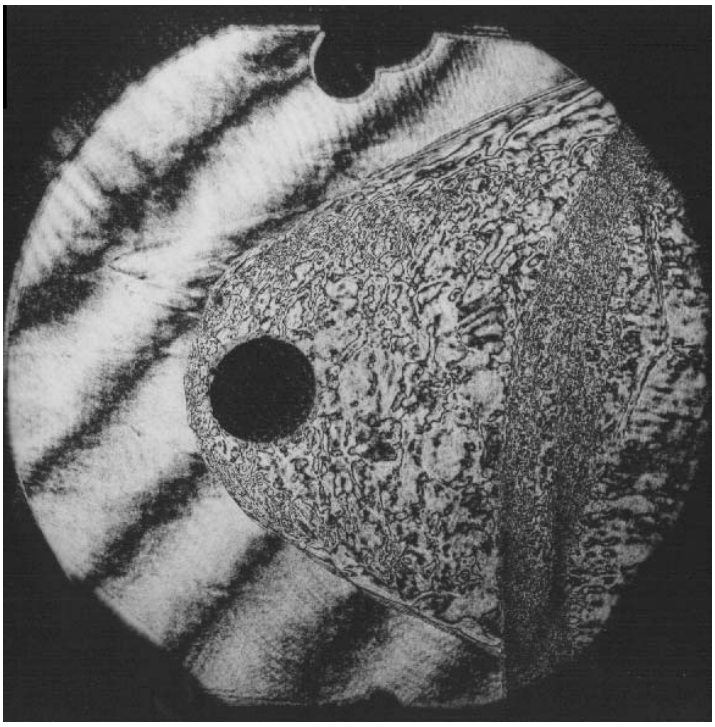

Figure 3.

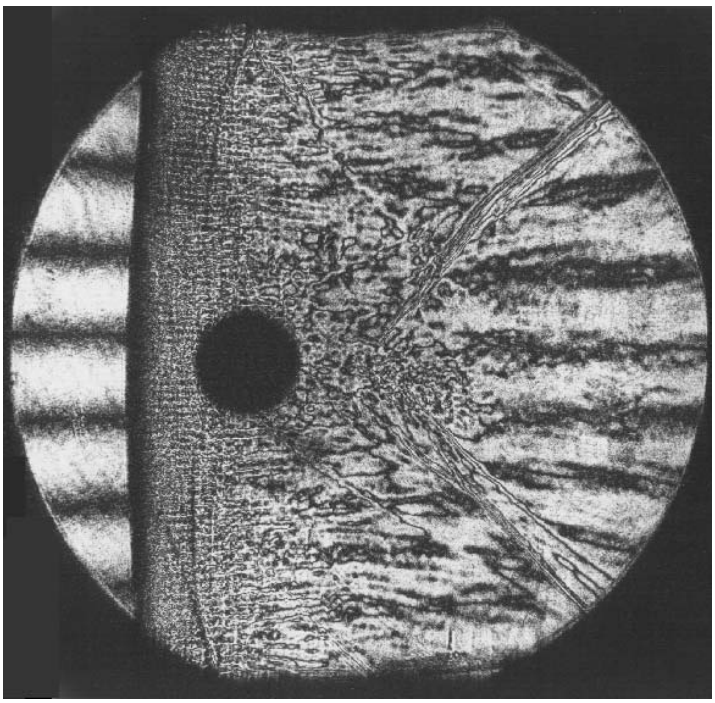

Figure 4.

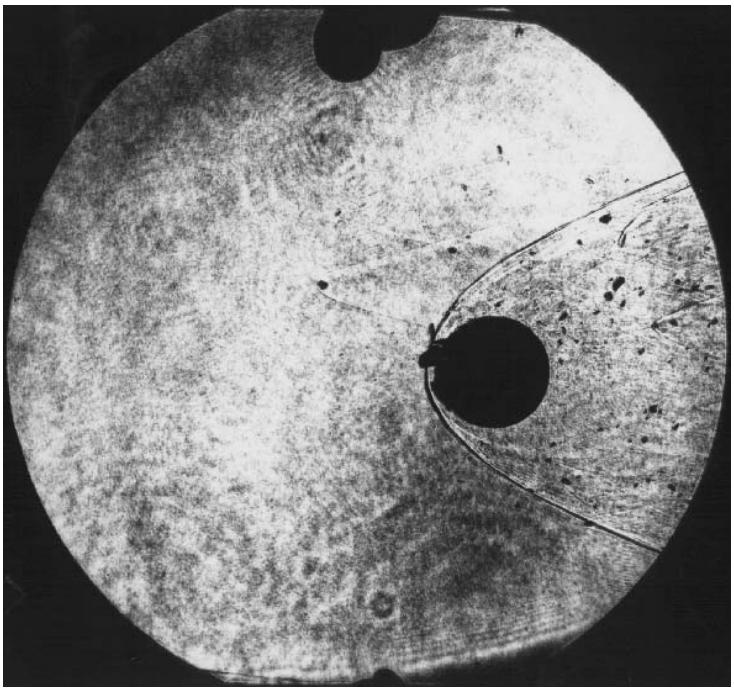

Figure 5.

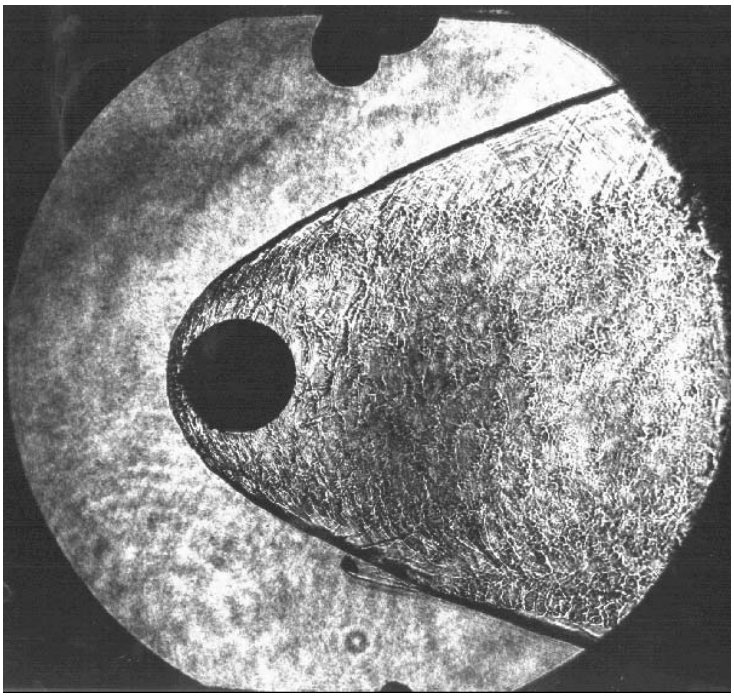

Figure 6.

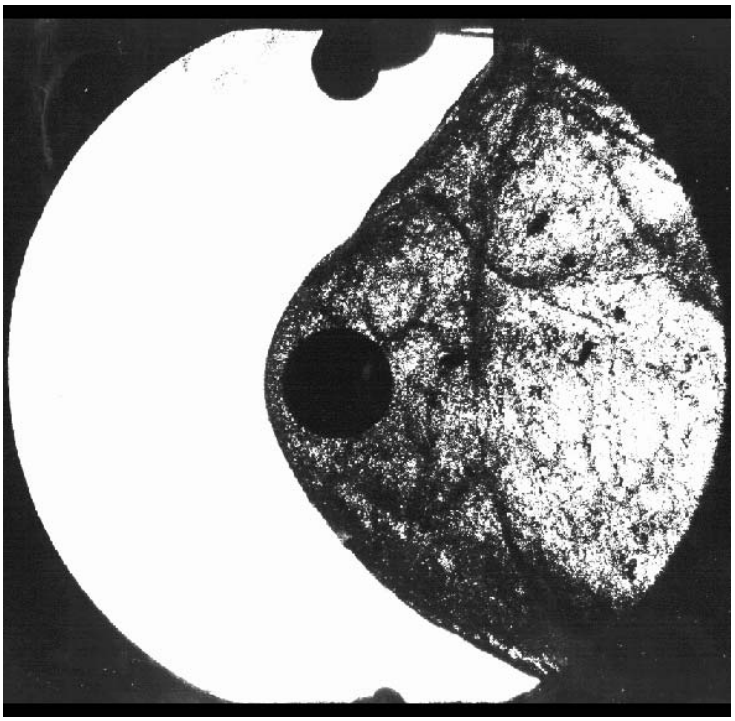

Figure 7.

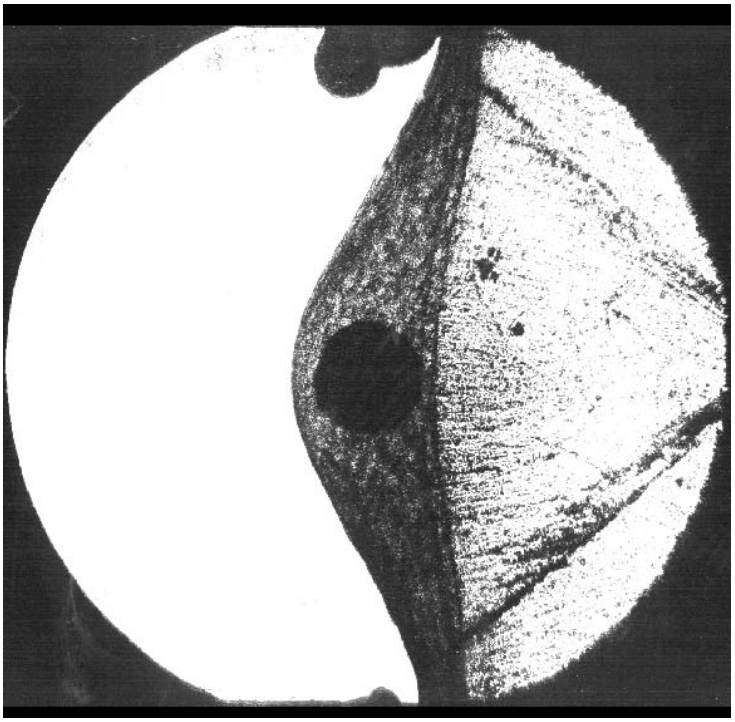

Figure 8.